Title:

***Nicotiana tabacum* contains two alpha1,3-fucosyltransferase types, one of which is able to catalyze core fucosylation of high-mannose *N*-glycans**

Authors:

Catherine Navarre[1], Nicolas Bailly[1], Juliette Balieu[2], Olivier Perruchon[2], Xavier Herman[1], Antoine Mercier[1], Adeline Courtoy[1], Patrice Lerouge[2], Muriel Bardor[2] & François Chaumont[1]

1 Louvain Institute of Biomolecular Science and Technology (LIBST), UCLouvain, Louvain-la-Neuve, Belgium

2 Université de Rouen Normandie, Normandie Univ, GlycoMEV UR 4358, SFR Normandie Végétal FED 4277, Innovation Chimie Carnot, IRIB, GDR CNRS Chémobiologie, Rouen, France

Corresponding authors:

Catherine Navarre
LIBST/FYMO/UCLouvain
Croix du sud 4-5/L7.07.14
1348 Louvain-la-Neuve
Belgium
catherine.navarre@uclouvain.be

François Chaumont
LIBST/FYMO/UCLouvain
Croix du sud 4-5/L7.07.14
1348 Louvain-la-Neuve
Belgium
francois.chaumont@uclouvain.be

Running Title:

GnTI-independent core fucosylation in plants

Keywords:

core fucosylation/ GnTI/ *N*-glycosylation/ *Nicotiana tabacum* BY-2/ plant alpha1,3-fucosyltransferase

Supplementary Data Included: Figs. S1 - S3

Abstract

N-glycosylation is a critical quality attribute to consider when expressing recombinant glycoproteins in eukaryotic cells including plant cells. *N*-acetylglucosaminyltransferase I (GnTI) initiates complex *N*-glycan maturation in the Golgi apparatus by transferring a single *N*-acetylglucosamine (GlcNAc) residue on the alpha1,3-arm of a Man5 *N*-glycan acceptor. This step is required for the processing of high mannose into hybrid and complex *N*-glycans. Therefore, Arabidopsis mutants lacking GnTI activity display accumulation of Man5 *N*-glycans instead of complex *N*-glycans and do not synthesise *N*-glycans containing core alpha1,3-fucose residue. In contrast, *GnTI* knock out cell line of *Nicotiana tabacum* BY-2 still displays a little core alpha1,3-fucose signal on western blotting. Here, we show that *N. tabacum* contains two alpha1,3-fucosyltransferase types, one of which is able to transfer a core alpha1,3-fucose on a Man5 substrate when no Man5Gn substrate is available such as in BY-2 *GnTI* knock-out cell lines.

Introduction

In plants and some invertebrates, GDP-L-Fuc:Asn-linked GlcNAc alpha1,3-fucosyltransferase activity of the GT10 family (EC 2.4.1.214) catalyzes the transfer of a L-fucose from GDP-L-fucose to the innermost asparagine-linked GlcNAc of *N*-glycans, forming an alpha1,3-linkage (Both, P., Sobczak, L., et al. 2011). The resulting core alpha1,3-fucose is an abundant non-human carbohydrate epitope that contributes to the potential immunogenicity of plant-made pharmaceuticals. To prevent its presence, it is important to know the exact specificities of the plant alpha1,3-fucosyltransferases (alpha1,3-FucTs) and so to facilitate the prediction of the fucosylation status of recombinant glycoproteins produced in plants. For instance, some plant alpha1,3-FucTs can use the structurally related UDP-L-galactose as a donor substrate in case of GDP-L-fucose shortage (Kogelmann, B., Palt, R., et al. 2023, Ohashi, H., Ohashi, T., et al. 2017, Rayon, C., Cabanes-Macheteau, M., et al. 1999).

GnTI has a key role in the formation of *N*-glycan diversity because it is responsible for the addition of a first single *N*-acetylglucosamine (GlcNAc) residue on the alpha1,3-arm of Man5 (Supplementary Figure 1). Addition of this particular residue on a Man5 is considered as a strict prerequisite before being further modified by Golgi alpha-mannosidase II, *N*-acetylglucosaminyltransferase II, beta1,2-xylosyltransferase, and alpha1,3-fucosyltransferase to form hybrid, complex and paucimannosidic *N*-glycans (Strasser, R. 2016). Impairing the synthesis of hybrid and complex *N*-glycans by knockdown or knockout of GnTI enzyme has been obtained for several plant species (Strasser, R. 2022). Arabidopsis complex glycan-deficient *cgl* mutants that lack GnTI activity were first described more than three decades ago (Von Schaewen, A., Sturm, A., et al. 1993). Since knockdown of GnTI activity did not suppress totally the formation of complex *N*-glycans (Strasser, R., Altmann, F., et al. 2004a), *GnTI* knockout lines are required to decipher the accepted substrates of downstream enzymes like alpha1,3-FucTs.

Inactivation of the two *GnTI* genes in *Nicotiana tabacum* Bright Yellow 2 (BY-2) suspension cells using CRISPR/Cas9 gene edition generated a cell line producing only high-mannose *N*-glycans, mainly Man5 and Man4 *N*-glycan structures (Herman, X., Far, J., et al. 2021). However, a very weak alpha1,3-fucose signal was still observed in the BY-2 *GnTI*-KO cell lines by western blotting using anti-alpha1,3-fucose antibodies (Herman, X., Far, J., et al. 2021). This specific signal disappeared in the *GnTI/FucT*-KO cell lines (Herman, X., Far, J., et al. 2021), suggesting that it corresponds to a structure depending on alpha1,3-fucosyltranferase activities.

The first plant alpha1,3-FucT protein was purified from mung bean seedlings and showed *in vitro* activity in the presence of GDP-Fucose, divalent cations like Mn^{2+} or Zn^{2+}, and *N*-glycopeptides bearing *N*-glycan structure like GnGn and Man5Gn (Leiter, H., Mucha, J., et al. 1999, Staudacher, E., Dalik, T., et al. 1995). No transfer of fucose was observed when the terminal GlcNAc residue was absent, suggesting that the terminal GlcNAc on the 3-linked mannose is a structural requirement for core plant alpha1,3-FucTs. It has been reported that the addition of the 6-arm non-reducing beta1,2-GlcNAc residue by GnTII is facilitated by the presence of the core alpha1,3-fucose residue (Yoo, J.Y., Ko, K.S., et al. 2015). In *A. thaliana*, two genes encode for core alpha1,3-FucT: *AtFucTA* (FUT11/AT3G19280) and *AtFucTB* (FUT12/AT1G49710) (Bakker, H., Schijlen, E., et al. 2001, Wilson, I.B.H., Rendić, D., et al. 2001). *In vitro* enzyme activity was first detected only for AtFucTA (Bakker, H., Schijlen, E., et al. 2001, Wilson, I.B.H., Rendić, D., et al. 2001), but finally both AtFucTA and AtFucTB seem to be active *in vivo* since inactivation of both genes was necessary to completely abolish core alpha1,3-fucosylation (Strasser, R., Altmann, F., et al. 2004b, Yoo, J.Y., Ko, K.S., et al. 2015).

In *N. tabacum*, there are four alpha1,3-FucT genes that cluster in two groups, each containing an isoform derived from the genome *Nicotiana sylvestris* (S-genome) and an isoform from *Nicotiana tomentosiformis* (T-genome) (Göritzer, K., Grandits, M., et al. 2022, Hanania, U., Ariel, T., et al. 2017, Mercx, S., Smargiasso, N., et al. 2017). This is also the case in *N. benthamiana*, another allotetraploid species (Jansing, J., Sack, M., et al. 2019). Phylogenetic analysis of the alpha1,3-FucT proteins from *N. tabacum* and *N. benthamiana* confirmed the presence of the two clusters, one containing NbFucT1, NbFucT2, NtFucTA and NtFucTB (group 2 in (Hanania, U., Ariel, T., et al. 2017)), and the other containing NbFucT3, NbFucT4, NtFucTC and NtFucTD (group 1 in (Hanania, U., Ariel, T., et al. 2017)) (Figure 1). The inactivation of *NbFucT1* and *NbFucT2* by TALEN did not abolish completely alpha1,3-FucT activity in *N. benthamiana* (Li, J., Stoddard, T.J., et al. 2016), suggesting that both clusters are important. Likewise, knock-out of all four *FucT* genes resulted in no core alpha1,3-fucose epitope on endogenous and recombinant glycoproteins produced in *N. tabacum* and *N. benthamiana* (Göritzer, K., Grandits, M., et al. 2022, Hanania, U., Ariel, T., et al. 2017, Jansing, J., Sack, M., et al. 2019, Kogelmann, B., Melnik, S., et

al. 2024, Mercx, S., Smargiasso, N., et al. 2017). NtFucTs display a topology typical of Golgi glycosyltransferases with a cytosolic N-terminal, a transmembrane and stem (CTS) region followed by a large globular catalytic domain with potential *N*-glycosylation sites and a plant particular C-terminal tail of about 100 residues that is essential for the enzyme activity (Supplementary Figure 2).

To investigate the origin of the puzzling alpha1,3-fucose signal observed in BY-2 *GnTI*-KO cell lines, separate knock-in of one *NtFucT* member from the two different clusters were carried out in *GnTI*/*FucT*-KO BY-2 cells. Thereby, we were able to identify the isoform responsible for the weak alpha1,3-fucose signal detected in *GnTI*-KO cell lines. In addition, overexpression of *NtFucTC* enabled the detection of the alpha1,3-fucosylated Man5F^{3} *N*-glycan structure by mass spectrometry. Altogether, these results provide new insights into the substrate specificity of plant alpha1,3-FucTs.

Results

Excision of the T-DNA in GnTI/FucT-KO cell lines

Direct knock-in of alpha1,3-FucT genes could not be carried out in the *GnTI/FucT*-KO BY-2 cell lines because the ectopic *NtFucT* transgene would have been targeted by the CRISPR-Cas9 machinery that was continuously expressed in the *GnTI*/*FucT*-KO cell lines. Introduction of silent mutations to suppress the PAM sequences in the *NtFucT* transgenes was considered, but such mutations were not feasible. Similarly, optimization of nucleotide sequences to mutate the three target sequences was not adopted, as we preferred to preserve the original nucleotide sequences.

Instead, we decided to remove the whole T-DNA used to generate the *GnTI/FucT*-KO cell lines (Figure 2A), applying an excision system based on the Cre recombinase-loxP strategy as the T-DNA contained loxP sites at both T-DNA borders as well as a cytosine deaminase (codA) negative selectable cassette (Figure 2A). Expression of the conditional toxic gene *codA* made plant cells sensitive to 5-fluorocytosine (5-FC). The binary plasmid pPZP-hpt-cre, which contained the Cre recombinase expression cassette and a hygromycin resistance marker, was used to transform the *GnTI*/*FucT*-KO #10 cell line obtained previously (Herman, X., Far, J., et al. 2021). Selection on medium containing hygromycin B (50 µg/mL) was followed by screenings with media supplemented with 5-FC (200 µg/mL). The parental cell line *GnTI*/*FucT*-KO#10 did not grow on hygromycin B- and 5-FC media. Fourteen out of eighteen *GnTI/FucT*-KO *Cre* cell lines grew well on 5-FC medium, and nine cell lines were then grown in liquid medium supplemented with 5-FC (100 µg/mL) and genomic DNA extracted and analyzed.

A PCR control, targeting *XylT*, was carried out using primers [XylTF and XylTR] and confirmed the presence of this gene in all genomic DNA samples (Figure 2B). Next, the presence of the C*as9* transgene was assessed using primers [Cas9F and NosR]. The expected 2 kb amplification was detected in all *GnTI*/*FucT*-KO control samples, while *GnTI*/*FucT*-KO-*Cre* samples did not display any signal, indicating excision of the transgene (Figure 2B). To characterize the remaining T-DNA sequence that should consist of a single loxP flanked by LB and RB, PCR amplification using primers located next to LB and RB [RecF and RecR] was tested. As expected, a 130 bp amplification was detected in all nine Cre-containing cell lines (Figure 2B). Sequencing of the small amplicon confirmed the suppression of the T-DNA between the two loxP sites, leaving only one loxP sequence flanked by the RB and LB. These results validated the efficacy of Cre-loxP-mediated recombination in *GnTI*/*FucT*-KO-*Cre* cell lines, resulting in excision of the *Cas9* transgene and *FucT*-specific gRNAs that would interfere with ectopic expression of *NtFucT* transgenes. To corroborate this at the protein level, we analyzed the presence of Cas9-Flag in protein samples derived from the parental *GnTI/FucT*-KO#10 and the *GnTI/FucT*-KO-*Cre*#10-16 cell lines by western blotting using anti-Flag antibodies (Figure 2C). A band at the expected size (164 kDa) was identified in the parental line, and not in the *GnTI/FucT*-KO-*Cre*#10-16.

Characterization of FucTs genomic edition in *the GnTI-FucT*-KO-*Cre*#10-16 cell line

The four *NtFucT* genes had been targeted in three different highly conserved sequences located in exon 3 by six different sgRNAs (Herman, X., Far, J., et al. 2021, Mercx, S., Smargiasso, N., et al. 2017). To characterize the mutations in the *NtFucT* loci of the *GnTI/FucT*-KO-Cre #10-16 line that was selected for ectopic expression of *NtFucTs*, we amplified the targeted regions followed by Sanger sequencing (Figure 3).

First, *NtFucTA* and *NtFucTB* were simultaneously amplified by PCR using primers [AB Fwd and AB Rev]. A single band of around 800 bp was detected after gel electrophoresis (data not shown). The PCR fragment was then purified and sequenced with a specific primer of *NtFucTB* [B Fwd]. Only the *NtFucTB* gene was sequenced, resulting in two different edition events (Figure 3). Similarly, the same PCR fragment was sequenced with the reverse primer A, but this resulted in both *NtFucTA* and *NtFucTB* sequences. Yet, due to the already identified editions for *NtFucTB*, we identified a single homogenous edition of *NtFucTA*.

NtFucTC and *NtFucTD* were simultaneously amplified by PCR using primers [CD Fwd and CD Rev]. Two bands (300 bp and 200 bp) were detected after gel electrophoresis and purified separately. The two bands were sequenced with CD Fwd and CD reverse 1. The 200 bp amplicon corresponded to a homogenous edition of *NtFucTC*. The 300 bp amplicon was heterogenous, but two different editions of *NtFucTD* could be identified (Figure 3).

This confirms that all four *NtFucT* genes were inactivated in the *GnTI/FucT*-KO-Cre #10-16 line by major INDELs at each targeted site in Exon 3, that resulted in early stop codons (Supplementary Figure 3). This feature was very similar to the editions observed in *XylT/FucT*-KO (Mercx, S., Smargiasso, N., et al. 2017), without showing exactly the same INDELs. In contrast, the editions observed by (Göritzer, K., Grandits, M., et al. 2022) with the same sgRNAs in *N. tabacum* SR-1 plants consisted only of 1 bp INDELs in sites 1 or 2, with no edition in site 3.

Overexpression of *NtFucTB* and *NtFucTC* in the *GnTI-FucT*-KO-*Cre* #10-16 cell line

Due to the similarity (>95% identity) between NtFucTA and NtFucTB on the one hand, and between NtFucTC and NtFucTD on the other hand, the coding sequences of *NtFucTB* or *NtFucTC*, which derive from the *N. tomentosiformis* ancestor, were cloned under the control of the strong constitutive CaMV *35S* promoter. To facilitate protein detection, both *NtFucT* cDNAs were fused at their C-terminus to a sequence encoding a Flag tag, as it was reported that the addition of a V5 tag to the C-terminus of the alpha1,3-FucT from the diatom *Phaeodactylum triconutum* did not impair its activity (Zhang, P., Burel, C., et al. 2019). The constructs were introduced into the *GnTI/FucT*-KO-*Cre* #10-16 line to generate transgenic cell lines expressing only *NtFucTB* or *NtFucTC*. A band around 65 kDa corresponding to NtFucTB-Flag or NtFucTC-Flag was specifically detected in the microsomal fraction of five FucTC and six FucTB transgenic cell lines (Figure 4A). The expression levels were similar for *NtFucTB* and *NtFucTC*.

The presence of glycoproteins bearing alpha1,3-fucosylated *N*-glycans in the nine transgenic cell lines was investigated by western blotting of TSP with specific anti-alpha1,3-fucose antibodies. The background signal from transgenic cell lines expressing *NtFucTB* was similar to that from the parental *GnTI/FucT*-KO-*Cre* #10-16. However, a much stronger signal was detected in the five cell lines expressing *NtFucTC* (Figure 4B). This alpha1,3-fucose signal was also well detected when the extracellular medium of some FucTC transgenic cell lines was analyzed (Figure 4C). This result suggests that only NtFucTC is capable of transferring alpha1,3-fucose to high mannose *N*-glycans.

The *N*-glycans decorating the secreted glycoproteins were then analyzed by MALDI-TOF mass spectrometry (Figure 5). A very similar *N*-glycome was obtained for *GnTI/FucT*-KO-*Cre* #10-16 and both FucTC#1 and FucTC#7 after PNGase A treatment, with mainly Man5 (80%) and Man4 (10%) structures. The remaining structures were all high mannose structures going from Man3 to Man9. However, an ion at *m/z* 1523, which probably corresponds to an alpha1,3-fucosylated $Man5F^3$ structure, was detected in both FucTC#1 and FucTC#7 cell lines (Figure 5 B-C1), while this ion was totally absent in the *GnTI/FucT*-KO-*Cre* #10-16 sample (Figure 5 A). Interestingly, no ion peak at *m/z* 1523 could be detected after treatment with PNGase F of FucTC#7 sample, indicating that this signal corresponded probably to an alpha1,3-linked core fucose (Figure 5 C2).

Expression of *NtFucTB* and *NtFucTC* in *XylT-FucT*-KO *N. benthamiana* leaves

To test the activity of NtFucTB and NtFucTC in a cell line containing the GnTI activity, we expressed both *NtFucTB* and *NtFucTC* constructs in a *FucT/XylT*-KO background *i.e.* in *N. benthamiana FucT/XylT*-KO leaves. The *N. benthamiana FucT/XylT*-KO#20-4 plant had been obtained previously (Jansing, J., Sack, M., et al. 2019) and found to be inactivated for all four *NbFucT* loci. Inactivation of *NbFucT1* and *NbFucT2* was achieved using three different sgRNA sequences (F3, F4, F5), while the fourth sgRNA (F7) matched a conserved sequence in Exon 4 of all four *NbFucTs* (Jansing, J., Sack, M., et al. 2019). We demonstrated by western blotting analysis that Cas9-Flag was expressed in leaf of *N. benthamiana FucT/XylT*-KO#20-4, indicating that the CRISPR/Cas9 machinery was still present in this line (Figure 6A). This implies that sgRNA sequences F3, F4 and F7, which match sequences in *NtFucTB* and *NtFucTC*, could impair the expression of these two constructs in *N. benthamiana FucT/XylT*-KO#20-4 leaves. Nonetheless, transient expression of *NtFucTB-Flag* and *NtFucTC-Flag* was carried out in *N. benthamiana FucT/XylT*-KO#20-4 leaves and resulted in the detection of a similar band corresponding to the alpha1,3-FucT size (around 65 kDa) in the microsomal fractions prepared from leaves infiltrated with both constructs (Figure 6B). Analysis of alpha1,3-fucosylated glycoproteins by western blotting of TSP with anti-alpha1,3-fucose antibodies showed that both NtFucT isoforms were capable of transferring alpha1,3-fucose onto complex *N*-glycans (Figure 6C).

Discussion

Excision of the CRISPR-Cas9 construct from the *GnTI-FucT*-KO genome was achieved by the expression of the Cre recombinase, which targeted the two loxP sequences flanking the T-DNA. Removal of the 14.5 kb insert was confirmed by growth in 5-FC supplemented medium, PCR assay and western blot analysis. Another elegant strategy for self-removal of the CRISPR-Cas9 T-DNA was recently documented (Sheva, M., Hanania, U., et al. 2020). This method combined T-DNA auto-excision following inducible expression of a specific sgRNA gene targeting the Z sequences located near both T-DNA borders and the use of the same negative CodA marker as we used.

The four *N. tabacum* alpha1,3-FucT proteins are grouped into two clusters (Hanania, U., Ariel, T., et al. 2017, Mercx, S., Smargiasso, N., et al. 2017). *N. tabacum* is an allotetraploid that is considered to originate from a hybridization event between ancestors of *N. sylvestris* and *N. tomentosifomis*. In both clusters, one isoform is derived from each ancestor: NtFucTA and NtFucTD from *N. sylvestris*, and NtFucTB and NtFucTC from *N. tomentosiformis* (Göritzer, K., Grandits, M., et al. 2022, Mercx, S., Smargiasso, N., et al. 2017). We tested the alpha1,3-FucT activity of the member from the T-genome of each group (NtFucTB and NtFucTC) in two different genetic backgrounds to evaluate their activity on specific *N*-glycan substrates.

We found that NtFucTC-Flag, but not NtFucTB-Flag, was capable of adding a core alpha1,3-fucose on Man5 *N*-glycans in *GnTI-FucT*-KO BY-2 cells with very low efficiency. On the other hand, both isoforms were able to transfer a core alpha1,3-fucose onto *N*-glycans of endogenous leaf proteins of *N. benthamiana FucT/XylT*-KO#20-4 (Jansing, J., Sack, M., et al. 2019), suggesting that alpha1,3-FucT from both groups can add a core alpha1,3-fucose onto *N*-glycans with the terminal GlcNAc on the 3-linked mannose and that do not contain xylose. This goes along the same lines as previous observations. *N*-glycan analysis of proteins derived from the *XylT*-KO *N. tabacum* BY-2 cell lines showed the presence of complex *N*-glycans containing alpha1,3-fucose residues (Hanania, U., Ariel, T., et al. 2017). Similarly, *N*-glycans containing alpha1,3-fucose were detected in *N. benthamiana* and *A. thaliana XylT*-KO plants (Jansing, J., Sack, M., et al. 2019, Kajiura, H., Okamoto, T., et al. 2012, Strasser, R., Altmann, F., et al. 2004b). This was also observed in *N. benthamiana XylT/FucT*-KD plants co-expressing an IgG with the maize alpha1,3-FucT (Castilho, A., Gruber, C., et al. 2015). Alpha1,3-FucT from *Mangifera indica* was also capable of transferring a core alpha1,3-fucose to bi-antennary glycans, whether or not a core alpha1,6-fucose residue was present (Okada, T., Ihara, H., et al. 2019).

The particular Man5F^3 *N*-glycan detected in the present study was also observed in an Arabidopsis *cgl1* mutant that displayed a small residual GnTI activity. For example, glucocerebrosidase and iduronidase produced in Arabidopsis *cgl1* seeds exhibited 3.1% and 0.4% Man5F^3, respectively (He, X., Galpin, J.D., et al. 2012, He, X., Pierce, O., et al. 2013). More precisely, some Man4F^3 and Man5F^3 structures were specifically detected on a single specific Asn451 on iduronidase purified from *cgl1* seeds (Pierce, O.M., McNair, G.R., et al. 2017). In comparison, no such Man5F^3 *N*-glycan was detected on acid alpha-glucosidase nor acid beta-glucosidase produced in rice *gnt1* T-DNA insertion suspension cultures (Jung, J.W., Choi, H.Y., et al. 2019, Jung, J.W., Huy, N.X., et al. 2017). The presence of a small proportion of Man5F^3 *N*-glycans in the FucTC-Flag BY-2 cell lines was probably related to a relaxed substrate affinity of NtFucTC for Man5, which is the main *N*-glycan present in the *GnTI-FucT*-KO derived cell lines. This clearly corresponds to an artificial *in vivo N*-glycosylation condition that could force Man5 to be an acceptor of NtFucTC. The core alpha1,3-fucosyltransferase from *C. elegans* was able to convert *in vitro* MM and MMF^6 glycopeptides to MMF^3 and MMF^{3}F^6, and Man5 glycopeptide was also weakly fucosylated (Both, P., Sobczak, L., et al. 2011). This suggests that some core alpha1,3-FucTs like NtFucTC tolerate a *N*-glycan without a beta1,2-linked GlcNAc within the acceptor substrate pocket.

It was also generally accepted that mammalian alpha1,6-FucT could transfer a core fucose to the innermost GlcNAc of a glycan if a GlcNAc had previously been transferred in a beta1,2 linkage onto the three-arm mannose residue of the Man5 intermediate by GnTI. However, several *in vivo* studies in GnTI-deficient CHO and HEK293 cell lines reported the presence of core alpha1,6-fucose on structures lacking the GlcNAc on the alpha1,3-mannose branch (Crispin, M., Harvey, D.J., et al. 2006, Lin, A.I., Philipsberg, G.A., et al. 1994, Yang, Q. and Wang, L.X. 2016). These results contradicted *in vitro* studies that showed no core alpha1,6-fucose for Man5 or Man4 free glycans incubated with Golgi-enriched membranes from porcine liver (Longmore, G.D. and Schachter, H. 1982)

or with purified human FUT8 enzyme (Li, L., Liu, Y., et al. 2015, Voynow, J.A., Kaiser, R.S., et al. 1991). Recent *in vitro* studies confirmed that core alpha1,6-fucosylation of free high-mannose glycans was not possible but clearly demonstrated that Man5 glycan could be efficiently core-fucosylated by FUT8 in an appropriate protein/peptide context around the *N*-glycosylation site (García-García, A., Serna, S., et al. 2021, Yang, Q., Zhang, R., et al. 2017).

The sequence identity between NtFucTB and NtFucTC is around 79%. The lack of the relaxed affinity for Man5 *N*-glycan observed for NtFucTB was probably related to small differences in the structure between the acceptor-binding region in NtFuctB and NtFucTC. The PDB structures of NtFucTB and NtFucTC were generated using the AlphaFold2 ColabFold server (Mirdita, M., Schütze, K., et al. 2022) and showed high prediction confidence (predicted Template Modelling score pTM>0.5, and predicted Local Distance Difference Test pLDDT>70). The structures with the highest rank (pLDDT ~ 85 and pTM~0.77) were selected and the orientation of the side chains was refined using GalaxyRefine (https://galaxy.seoklab.org/cgi-bin/submit.cgi?type=REFINE). The structures were aligned with several crystalized GT10 alpha1,3/alpha1,4-fucosyltransferase structures that generate different Lewis antigens (*Helicobacter pylori*: 2NZY, *Magnifera indica*: 7YRO and human: 8D0Q). The different proteins aligned very well on the GDP-fucose binding domain and on the position of the catalytic glutamate. The other domains poorly aligned, possibly because of differences in the substrate specificity. Next, the glycan conformer corresponding to Asn- Man5Gn was generated using Glycam (https://glycam.org) and then docked into the catalytic pocket using DockingPie 1.2 (Rosignoli, S. and Paiardini, A. 2022). The acceptor substrate pockets of NtFucTB and NtFucTC are very similar with many hydrophilic residues able to make contacts with the glycan (Figure 7). The main difference lies at the distal region from the catalytic site: the HGPGQELK sequence of NtFucTB is replaced by HGGEKDWK in NtFucTC. Our hypothesis is that the position of the acceptor glycan inside the pocket must be tightly controlled to enable efficient transfer of the fucose to the first core GlcNAc residue, and that this is the case for a Man5Gn acceptor in NtFucTB and NtFucTC. We postulate that the pocket of NtFucTC could still accommodate and modify a Man5 glycan, albeit less efficiently than the Man5Gn substrate, whereas this is not the case for the pocket of NtFucTB.

Finally, it is also interesting to note that the expression of NtFucTB-Flag and NtFucTC-Flag in *N. benthamiana* leaves was successful despite the presence of the CRISPR/Cas9 machinery, which is expected to target *NbFucT* sequences that are partially present in the expressed *NtFucT* genes. This is probably linked to the high production of both NtFucT proteins under agroinfiltration for a limited period (4 days post infiltration).

In conclusion, our data show that Man5 can serve as a substrate, albeit to a lesser extent than Man5Gn, for the tobacco alpha1,3-FucT from group 1, but not from group 2. This supports the presence of a GnTI-independent core fucosylation pathway, at least in *GnTI*-KO BY-2 cells. Better knowledge of underlying alpha1,3-FucT activities is important when manufacturing therapeutic glycoproteins in plants since the production of some recombinant proteins may end with a low presence of $Man5F^3$ on some N-glycosites.

Materials and Methods

Cre plasmid construction

The *Cre* expression cassette was generated using the modular plant transformation vectors pPZP-RCS/pAUX (Goderis, I.J.W.M., De Bolle, M.F.C., et al. 2002). The *Cre* nucleotide sequence was recovered by SmaI/HincII digestion from the yeast vector pSH47, which carries the *Cre* gene under the control of the inducible *GAL1* promoter (Güldener, U., Heck, S., et al. 1996), and inserted into the SmaI site of the pAUX3132-En2p35S-[KpnI-ScaI-XhoI-BamHI-SmaI-SacI]-tNOS. The Cre recombinase cassette under the control of the enhanced *CaMV 35S* promoter (*En2p35S*) and the nopaline synthase terminator (*tNOS*) was then inserted into the I-CeuI site of the pPZP-hpt binary vector (Herman, X., Far, J., et al. 2023).

NtFucT plasmid construction

The *NtFucT* expression cassettes were constructed using the Golden Gate Modular Cloning (MoClo) assembly method (Weber, E., Engler, C., et al. 2011) and DNA parts from the MoClo Plant toolbox (Engler, C., Youles, M., et al. 2014). The open reading frames (7 exons) of *NtFucTB* and *NtFucTC* flanked with the BsaI restriction site were synthesized (GenScript Biotech, Piscataway, NJ) and assembled with the enhanced cauliflower mosaic virus *35S* promoter (pICH51288), the sequence encoding the 3XFlag-tag in 3' (pICSL50007) and the nopaline synthase terminator (pICH41421) in a pICH47742 level 1 position 2 plasmid (*FucTB*) or a pICH47751 level 1 position 3 plasmid (*FucTC*). Two distinct level M constructs were obtained by assembling the kanamycin resistance cassette (pICH47732) with level 1 FucTB-Flag or level 1 FucTC-Flag.

N. tabacum BY-2 cell culture

BY-2 cell lines were grown in the dark at 25°C with agitation on a rotary shaker (90 rpm) in liquid MS medium [4.4 g/L Murashige and Skoog medium including vitamins (DUCHEFA Biochemie, M0222), 30 g/L sucrose, 0.2 g/L KH_2PO_4, 2.5 mg/L thiamine, 50 mg/L myo-inositol, and 0.2 mg/L 2,4-dichlorophenoxyacetic acid, pH 5.8 (KOH). Cultures were grown in 50 mL of medium in a 250 mL Erlenmeyer flask and an 8% inoculum was transferred each week into fresh medium.

BY-2 cell transformation and *N. benthamiana* leaf agroinfiltration

The vectors pPZP-hpt-Cre, GG-nptII-FucTB-Flag and GG-nptII-FucTC-Flag were transferred into *Agrobacterium tumefaciens* LBA4404virG (van der Fits, L., Deakin, E.A., et al. 2000) by electroporation. Transformation of BY-2 cells was carried out as described in (Navarre, C. and Chaumont, F. 2022). Hygromycin B resistance marker was used to select the *GnTI/FucT*-KO-*Cre* transgenics while kanamycin resistance gene was used to select the *GnTI/FucT*-KO-*Cre*-*FucTB* and GnTI/FucT-KO-Cre-*FucTC* transgenics. Selection of BY-2 transformed cell lines was carried out on MS-agar plates containing 50 µg/mL hygromycin or 100 µg/mL kanamycin, respectively. For agro-infiltration, *N. benthamiana FucT/XylT* KO#20-4 leaves were infiltrated on the abaxial side with a suspension of *A. tumefaciens* in infiltration medium (10 m MES, 10 mM $MgCl_2$, pH 5.6 (KOH)) at a final OD_{600} of 0.8. The plants were incubated in a phytotron with a 16/8-h day/night cycle at 24°C.

Analysis of genome modifications

Genomic DNA was extracted from BY-2 transgenic transformants using Wizard Genomic Purification kit following the instruction of the supplier (PROMEGA, A1120). PCR was performed using specific primers (Supplementary Table I) flanking the targeted regions. The PCR products were purified using PCR Clean-up kit (Macherey-Nagel, reference 740609) and the amplicons were sequenced by Sanger sequencing (Mycrosynth, Balgach, Switzerland). The sequences were analyzed by local alignment using CLC Main Workbench software (QIAGEN) and by frequency of targeted mutations using the TIDE algorithm version 3.3.0 (Brinkman, E.K., Chen, T., et al. 2014).

Protein Extracts

BY-2 cultures (2 mL) were filtered on three layers of Miracloth (MILLIPORE, reference 475855). Filtered BY-2 cells were homogenized in 700 µL buffer [250 mM sorbitol, 60 mM Tris–HCl, 2 mM Na_2EDTA, pH 8.0]

supplemented with 1 mM PMSF and 1 µg/ml protease inhibitor cocktail [leupeptin, aprotinin, antipain, pepsatin, chymostatin]) using 0.5 g of glass beads (0.85–1.23 mm) and a Precellys 24 tissue homogenizer (BERTIN Technologies, Montigny-le-Bretonneux, France). Crude extracts were centrifuged first at 2,800 *g* for 5 min, then at 10,000 *g* for 7 min. The supernatant was then centrifuged at 100,000 *g* for 15 min to recover the supernatant (TSP) and a pellet (microsomal fraction) that was resuspended by sonication in 5 mM KH_2PO_4 pH 7.8, 3 mM KCl, 330 mM sucrose. In case of nuclear proteins extraction, the cells were homogenized in 700 µl buffer (400 mM NaCl, 60 mM Tris–HCl, 2 mM Na_2EDTA, pH 8.0, supplemented with a protease inhibitor cocktail) and centrifuged first at 1,000 *g* for 5 min, then at 9,000 *g* for 10 min. The supernatant (total proteins) was collected.

Agro-infiltrated leaves (three disks of 60 mg) were collected at 4 dpi, frozen in liquid nitrogen and grinded in 700 µL of extraction [250 mM sorbitol, 60 mM Tris-HCl, 2 mM Na_2EDTA, 10 mM DTT, pH 8.0] supplemented with 0.6% Polyclar AT, 1 mM PMSF and 1 µg/ml protease inhibitor cocktail [leupeptin, aprotinin, antipain, pepsatin, chymostatin]. Grinding was performed on ice in a Potter-Elvehjem tissue homogenizer (KONTES GLASS, Vineland, NJ). Crude extracts were centrifuged first at 2,800 *g* for 5 min, then at 10,000 *g* for 7 min. The supernatant (total proteins) was then centrifuged at 100,000 *g* for 15 min to recover the supernatant (total soluble proteins, TSP) and a pellet (microsomal fraction) that was resuspended by sonication in 5 mM KH_2PO_4 pH 7.8, 3 mM KCl, 330 mM sucrose.

Immunoblot analysis

Protein concentrations were determined according to Bradford (1976) using BSA as a standard. Protein samples were resolved on 4%–20% polyacrylamide gel (GenScript, reference M00656) in Tris-MOPS-SDS buffer (GenScript, reference M00138) and transferred onto a 0.2 µm PVDF membrane (BIORAD, Trans-Blot Turbo Transfer Pack, reference 1704156) for western blotting. To detect Flag-tag on Cas9 or NtFucTB/C proteins, blots were incubated with 1:1,000 monoclonal anti-Flag M2-Alkaline Phosphatase antibody produced in mouse (SIGMA-ALDRICH, reference A9469) and alkaline phosphatase was detected using BM Purple AP substrate (ROCHE, reference 11442074001).

To examine the presence of glycans bearing core alpha1,3-fucose in the protein samples, blots were incubated with 1:5,000 rabbit anti-fucose antisera (AGRISERA, reference AS07268), followed by 1:10,000 peroxidase-conjugated monoclonal anti-rabbit antisera (SYNABS, reference LO-RG-1-HPRO). Detection was performed using Roche ECL substrate (GE Healthcare,).

N-glycans analysis

For the MS analysis, BY-2 cells were grown in 50 mL of MS medium in 250 mL Erlenmeyer flasks. Extracellular proteins were collected by filtration on three layers of Miracloth, then centrifuged at 8,000 *g* for 30 min, and precipitated by salting-out as previously described (Herman, X., Far, J., et al. 2021). The pellet was resuspended in 500 µL of PBS buffer and desalted on a PD MiniTrap G-10 column (CYTIVA, reference 28918010) equilibrated with PBS buffer.

For the analysis of the *N*-glycan profiles by PNGase A, proteins were lyophilized and then digested using Trypsin (PROMEGA, reference V511A in a ratio 1:20) in 100 mM ammonium bicarbonate pH 8 overnight at 37°C. Samples were heated at 100°C for 10 minutes in order to inactivate the Trypsin, followed by a 3 hours TLCK-treated chymotrypsin digestion (SIGMA, reference C3142, ratio 1:20) in 100 mM ammonium bicarbonate pH 8 at 37°C. Once again, the digested samples were heated at 100°C for 10 minutes in order to inactivate the Chymotrypsin prior to lyophilization. Then, *N*-glycans were released with 0.2 mU of PNGase A (AGILENT, reference GKE-5011B, ratio 0.5 mU / 2.5 mg of proteins) in 50 mM sodium acetate buffer pH 5 at 37°C overnight. For the analysis of the *N*-glycan profiles by PNGase F, proteins were denaturated using 0.1 % SDS in Tris Buffer 0.1 M pH 7.5 incubated for 5 min at 100 °C. Then, *N*-glycans were released with 1 U of N-glycosidase F (PNGase F; Roche, reference 11365177001) in Tris Buffer 0.1 M pH 7.5 + 0.5 % NP40 incubated at 37°C overnight. Four volumes of ethanol were added to the samples, then samples were frozen overnight and centrifugated at 10,000 g for 30 min.

Released *N*-glycans by PNGase A or PNGase F were then purified using C18 (THERMO FISHER, reference 60108-303) and carbograph cartridges (THERMO FISHER, reference 60106-301) according to the manufacturer's

instructions. Finally, released *N*-glycans were labelled at 60°C for 2 h with 0.35M 2-Aminobenzamide (THERMO SCIENTIFIC, reference A 14756) in DMSO/acetic acid (70/30, (v/v)) containing 1 M of sodium cyanoborohydrure (SIGMA, reference 156159-10G). Then, *N*-glycans were purified on Agilent S cartridges (AGILENT, reference GKI-4726) according to the manufacturer's instructions and analyzed by MALDI TOF mass spectrometry in positive ion mode (MALDI TOF-TOF ultrafleXtreme, Bruker Daltonics, Breme, Germany) as previously reported (Balieu, J., Jung, J.W., et al. 2022).

Acknowledgments

We are very grateful to Professor Stefan Schillberg and Dr. Nicole Raven from Fraunhofer Institute for Molecular Biology and Applied Ecology IME (Aachen, Germany) for providing us with the *Nicotiana benthamiana XylT/FucT* KO seeds. We acknowledge Dr. Claudio Screpanti and Dr. Emmanuel Van Cutsem for preliminary data with the Cre-loxP system in BY-2 cells. We are pleased to thank Professor Marc Boutry for his constant interest in our research and his careful reading of this manuscript. Nicolas Bailly and Xavier Herman were recipients of a fellowship from the Fonds pour la Formation à la Recherche dans l'Industrie et l'Agriculture (FRIA, Belgium). The University of Rouen Normandie's support is gratefully acknowledged. The work performed in the GlycoMEV lab, University of Rouen Normandie received financial funding from the French government through the ANR agency, both under the PIA Grand Défi Biomédicaments, PhaeomAbs project (ANR-21-F2II-0005) and the ANR PRCE DAGENTA project (ANR-21-CE20-0038-001).

Abbreviations

Glycan nomenclature according to (Altmann, F., Helm, J., et al. 2024).

References

Altmann F, Helm J, Pabst M, Stadlmann J. 2024. Introduction of a human- and keyboard-friendly N-glycan nomenclature. *Beilstein J Org Chem*, 20:607-620.

Bakker H, Schijlen E, de Vries T, Schiphorst WE, Jordi W, Lommen A, Bosch D, van Die I. 2001. Plant members of the alpha1-->3/4-fucosyltransferase gene family encode an alpha1-->4-fucosyltransferase, potentially involved in Lewis(a) biosynthesis, and two core alpha1-->3-fucosyltransferases. *FEBS Lett*, 507:307-312.

Balieu J, Jung JW, Chan P, Lomonossoff GP, Lerouge P, Bardor M. 2022. Investigation of the N-Glycosylation of the SARS-CoV-2 S Protein Contained in VLPs Produced in Nicotiana benthamiana. *Molecules*, 27:5119.

Both P, Sobczak L, Breton C, Hann S, Nöbauer K, Paschinger K, Kozmon S, Mucha J, Wilson IB. 2011. Distantly related plant and nematode core α1,3-fucosyltransferases display similar trends in structure-function relationships. *Glycobiology*, 21:1401-1415.

Brinkman EK, Chen T, Amendola M, van Steensel B. 2014. Easy quantitative assessment of genome editing by sequence trace decomposition. *Nucleic Acids Research*, 42:e168-e168.

Castilho A, Gruber C, Thader A, Oostenbrink C, Pechlaner M, Steinkellner H, Altmann F. 2015. Processing of complex N-glycans in IgG Fc-region is affected by core fucosylation. *mAbs*, 7:863-870.

Crispin M, Harvey DJ, Chang VT, Yu C, Aricescu AR, Jones EY, Davis SJ, Dwek RA, Rudd PM. 2006. Inhibition of hybrid- and complex-type glycosylation reveals the presence of the GlcNAc transferase I-independent fucosylation pathway. *Glycobiology*, 16:748-756.

Engler C, Youles M, Gruetzner R, Ehnert TM, Werner S, Jones JD, Patron NJ, Marillonnet S. 2014. A golden gate modular cloning toolbox for plants. *ACS Synth Biol*, 3:839-843.

García-García A, Serna S, Yang Z, Delso I, Taleb V, Hicks T, Artschwager R, Vakhrushev SY, Clausen H, Angulo J*, et al.* 2021. FUT8-Directed Core Fucosylation of N-glycans Is Regulated by the Glycan Structure and Protein Environment. *ACS Catalysis*, 11:9052-9065.

Goderis IJWM, De Bolle MFC, Francois IEJA, Wouters PFJ, Broekaert WF, Cammue BPA. 2002. A set of modular plant transformation vectors allowing flexible insertion of up to six expression units. *Plant Molecular Biology*, 50:17-27.

Göritzer K, Grandits M, Grünwald-Gruber C, Figl R, Mercx S, Navarre C, Ma JK, Teh AY. 2022. Engineering the N-glycosylation pathway of Nicotiana tabacum for molecular pharming using CRISPR/Cas9. *Front Plant Sci*, 13:1003065.

Guindon S, Dufayard J-F, Lefort V, Anisimova M, Hordijk W, Gascuel O. 2010. New Algorithms and Methods to Estimate Maximum-Likelihood Phylogenies: Assessing the Performance of PhyML 3.0. *Systematic Biology*, 59:307-321.

Güldener U, Heck S, Fielder T, Beinhauer J, Hegemann JH. 1996. A new efficient gene disruption cassette for repeated use in budding yeast. *Nucleic Acids Res*, 24:2519-2524.

Hanania U, Ariel T, Tekoah Y, Fux L, Sheva M, Gubbay Y, Weiss M, Oz D, Azulay Y, Turbovski A*, et al.* 2017. Establishment of a tobacco BY2 cell line devoid of plant-specific xylose and fucose as a platform for the production of biotherapeutic proteins. *Plant Biotechnol J*, 15:1120-1129.
He X, Galpin JD, Tropak MB, Mahuran D, Haselhorst T, von Itzstein M, Kolarich D, Packer NH, Miao Y, Jiang L*, et al.* 2012. Production of active human glucocerebrosidase in seeds of Arabidopsis thaliana complex-glycan-deficient (cgl) plants. *Glycobiology*, 22:492-503.
He X, Pierce O, Haselhorst T, von Itzstein M, Kolarich D, Packer NH, Gloster TM, Vocadlo DJ, Qian Y, Brooks D*, et al.* 2013. Characterization and downstream mannose phosphorylation of human recombinant α-L-iduronidase produced in Arabidopsis complex glycan-deficient (cgl) seeds. *Plant Biotechnol J*, 11:1034-1043.
Herman X, Far J, Courtoy A, Bouhon L, Quinton L, De Pauw E, Chaumont F, Navarre C. 2021. Inactivation of N-Acetylglucosaminyltransferase I and α1,3-Fucosyltransferase Genes in Nicotiana tabacum BY-2 Cells Results in Glycoproteins With Highly Homogeneous, High-Mannose N-Glycans. *Frontiers in plant science*, 12:634023-634023.
Herman X, Far J, Peeters M, Quinton L, Chaumont F, Navarre C. 2023. In vivo deglycosylation of recombinant glycoproteins in tobacco BY-2 cells. *Plant Biotechnol J*.
Jansing J, Sack M, Augustine SM, Fischer R, Bortesi L. 2019. CRISPR/Cas9-mediated knockout of six glycosyltransferase genes in Nicotiana benthamiana for the production of recombinant proteins lacking β-1,2-xylose and core α-1,3-fucose. *Plant Biotechnol J*, 17:350-361.
Jung JW, Choi HY, Huy NX, Park H, Kim HH, Yang MS, Kang SH, Kim DI, Kim NS. 2019. Production of recombinant human acid β-glucosidase with high mannose-type N-glycans in rice gnt1 mutant for potential treatment of Gaucher disease. *Protein Expr Purif*, 158:81-88.
Jung JW, Huy NX, Kim HB, Kim NS, Van Giap D, Yang MS. 2017. Production of recombinant human acid α-glucosidase with high-mannose glycans in gnt1 rice for the treatment of Pompe disease. *J Biotechnol*, 249:42-50.
Junier T, Zdobnov EM. 2010. The Newick utilities: high-throughput phylogenetic tree processing in the Unix shell. *Bioinformatics*, 26:1669-1670.
Kajiura H, Okamoto T, Misaki R, Matsuura Y, Fujiyama K. 2012. Arabidopsis β1,2-xylosyltransferase: Substrate specificity and participation in the plant-specific N-glycosylation pathway. *Journal of Bioscience and Bioengineering*, 113:48-54.
Katoh K, Standley DM. 2013. MAFFT Multiple Sequence Alignment Software Version 7: Improvements in Performance and Usability. *Molecular Biology and Evolution*, 30:772-780.
Kogelmann B, Melnik S, Bogner M, Kallolimath S, Stöger E, Sun L, Strasser R, D'Aoust MA, Lavoie PO, Saxena P*, et al.* 2024. A genome-edited N. benthamiana line for industrial-scale production of recombinant glycoproteins with targeted N-glycosylation. *Biotechnol J*, 19:e2300323.
Kogelmann B, Palt R, Maresch D, Strasser R, Altmann F, Kallolimath S, Sun L, D'Aoust MA, Lavoie PO, Saxena P*, et al.* 2023. In planta expression of active bacterial GDP-6-deoxy-d-lyxo-4-hexulose reductase for glycan modulation. *Plant Biotechnol J*, 21:1929-1931.
Leiter H, Mucha J, Staudacher E, Grimm R, Glössl J, Altmann F. 1999. Purification, cDNA cloning, and expression of GDP-L-Fuc:Asn-linked GlcNAc alpha1,3-fucosyltransferase from mung beans. *J Biol Chem*, 274:21830-21839.
Lemoine F, Correia D, Lefort V, Doppelt-Azeroual O, Mareuil F, Cohen-Boulakia S, Gascuel O. 2019. NGPhylogeny.fr: new generation phylogenetic services for non-specialists. *Nucleic Acids Research*, 47:W260-W265.
Li J, Stoddard TJ, Demorest ZL, Lavoie P-O, Luo S, Clasen BM, Cedrone F, Ray EE, Coffman AP, Daulhac A*, et al.* 2016. Multiplexed, targeted gene editing in Nicotiana benthamiana for glyco-engineering and monoclonal antibody production. *Plant Biotechnology Journal*, 14:533-542.
Li L, Liu Y, Ma C, Qu J, Calderon AD, Wu B, Wei N, Wang X, Guo Y, Xiao Z*, et al.* 2015. Efficient chemoenzymatic synthesis of an N-glycan isomer library. *Chemical Science*, 6:5652-5661.
Lin AI, Philipsberg GA, Haltiwanger RS. 1994. Core fucosylation of high-mannose-type oligosaccharides in GlcNAc transferase I-deficient (Lec1) CHO cells. *Glycobiology*, 4:895-901.
Longmore GD, Schachter H. 1982. Product-identification and substrate-specificity studies of the GDP-l-fucose: 2-acetamido-2-deoxy-β-d-glucoside (fuc→asn-linked GlcNAc) 6-α-l-fucosyltransferase in a golgi-rich fraction from porcine liver. *Carbohydrate Research*, 100:365-392.

Mercx S, Smargiasso N, Chaumont F, De Pauw E, Boutry M, Navarre C. 2017. Inactivation of the β(1,2)-xylosyltransferase and the α(1,3)-fucosyltransferase genes in Nicotiana tabacum BY-2 Cells by a Multiplex CRISPR/Cas9 Strategy Results in Glycoproteins without Plant-Specific Glycans. *Front Plant Sci*, 8:403.
Mirdita M, Schütze K, Moriwaki Y, Heo L, Ovchinnikov S, Steinegger M. 2022. ColabFold: making protein folding accessible to all. *Nature Methods*, 19:679-682.
Navarre C, Chaumont F. 2022. Production of Recombinant Glycoproteins in Nicotiana tabacum BY-2 Suspension Cells. *Methods Mol Biol*, 2480:81-88.
Ohashi H, Ohashi T, Kajiura H, Misaki R, Kitamura S, Fujiyama K. 2017. Fucosyltransferases produce N-glycans containing core l-galactose. *Biochemical and Biophysical Research Communications*, 483:658-663.
Okada T, Ihara H, Ikeda Y. 2019. Characterization of MiFUT11 from Mangifera indica L.: A functional core α1,3-fucosyltransferase potentially involved in the biosynthesis of immunogenic carbohydrates in mango fruit. *Phytochemistry*, 165:112050.
Pierce OM, McNair GR, He X, Kajiura H, Fujiyama K, Kermode AR. 2017. N-glycan structures and downstream mannose-phosphorylation of plant recombinant human alpha-L-iduronidase: toward development of enzyme replacement therapy for mucopolysaccharidosis I. *Plant Mol Biol*, 95:593-606.
Rayon C, Cabanes-Macheteau M, Loutelier-Bourhis C, Salliot-Maire I, Lemoine J, Reiter WD, Lerouge P, Faye L. 1999. Characterization of N-glycans from Arabidopsis. Application to a fucose-deficient mutant. *Plant Physiol*, 119:725-734.
Rosignoli S, Paiardini A. 2022. DockingPie: a consensus docking plugin for PyMOL. *Bioinformatics*, 38:4233-4234.
Sheva M, Hanania U, Ariel T, Turbovski A, Rathod VKR, Oz D, Tekoah Y, Shaaltiel Y. 2020. Sequential Genome Editing and Induced Excision of the Transgene in N. tabacum BY2 Cells. *Front Plant Sci*, 11:607174.
Staudacher E, Dalik T, Wawra P, Altmann F, März L. 1995. Functional purification and characterization of a GDP-fucose: beta-N-acetylglucosamine (Fuc to Asn linked GlcNAc) alpha 1,3-fucosyltransferase from mung beans. *Glycoconj J*, 12:780-786.
Strasser R. 2016. Plant protein glycosylation. *Glycobiology*, 26:926-939.
Strasser R. 2022. Recent Developments in Deciphering the Biological Role of Plant Complex N-Glycans. *Front Plant Sci*, 13:897549.
Strasser R, Altmann F, Glössl J, Steinkellner H. 2004a. Unaltered complex N-glycan profiles in Nicotiana benthamiana despite drastic reduction of beta1,2- N -acetylglucosaminyltransferase I activity. *Glycoconj J*, 21:275-282.
Strasser R, Altmann F, Mach L, Glössl J, Steinkellner H. 2004b. Generation of Arabidopsis thaliana plants with complex N-glycans lacking beta1,2-linked xylose and core alpha1,3-linked fucose. *FEBS Lett*, 561:132-136.
van der Fits L, Deakin EA, Hoge JHC, Memelink J. 2000. The ternary transformation system: constitutive virG on a compatible plasmid dramatically increases Agrobacterium-mediated plant transformation. *Plant Molecular Biology*, 43:495-502.
Von Schaewen A, Sturm A, O'Neill J, Chrispeels MJ. 1993. Isolation of a mutant Arabidopsis plant that lacks N-acetyl glucosaminyl transferase I and is unable to synthesize golgi-modified complex N-linked glycans. *Plant Physiology*, 102:1109-1118.
Voynow JA, Kaiser RS, Scanlin TF, Glick MC. 1991. Purification and characterization of GDP-L-fucose-N-acetyl beta-D-glucosaminide alpha 1-6fucosyltransferase from cultured human skin fibroblasts. Requirement of a specific biantennary oligosaccharide as substrate. *J Biol Chem*, 266:21572-21577.
Weber E, Engler C, Gruetzner R, Werner S, Marillonnet S. 2011. A modular cloning system for standardized assembly of multigene constructs. *PLoS One*, 6:e16765.
Wilson IBH, Rendić D, Freilinger A, Dumić J, Altmann F, Mucha J, Müller S, Hauser M-T. 2001. Cloning and expression of cDNAs encoding α1,3-fucosyltransferase homologues from Arabidopsis thaliana1The cDNA sequences referred to in this publication have been deposited with the EMBL database under the numbers AJ404860 (FucTA), AJ404861 (FucTB) and AJ404862 (FucTC).1. *Biochimica et Biophysica Acta (BBA) - General Subjects*, 1527:88-96.
Yang Q, Wang LX. 2016. Mammalian α-1,6-Fucosyltransferase (FUT8) Is the Sole Enzyme Responsible for the N-Acetylglucosaminyltransferase I-independent Core Fucosylation of High-mannose N-Glycans. *J Biol Chem*, 291:11064-11071.

Yang Q, Zhang R, Cai H, Wang LX. 2017. Revisiting the substrate specificity of mammalian α1,6-fucosyltransferase reveals that it catalyzes core fucosylation of N-glycans lacking α1,3-arm GlcNAc. *J Biol Chem*, 292:14796-14803.
Yoo JY, Ko KS, Seo HK, Park S, Fanata WI, Harmoko R, Ramasamy NK, Thulasinathan T, Mengiste T, Lim JM*, et al.* 2015. Limited Addition of the 6-Arm β1,2-linked N-Acetylglucosamine (GlcNAc) Residue Facilitates the Formation of the Largest N-Glycan in Plants. *J Biol Chem*, 290:16560-16572.
Zhang P, Burel C, Plasson C, Kiefer-Meyer M-C, Ovide C, Gügi B, Wan C, Teo G, Mak A, Song Z*, et al.* 2019. Characterization of a GDP-Fucose Transporter and a Fucosyltransferase Involved in the Fucosylation of Glycoproteins in the Diatom Phaeodactylum tricornutum. *Frontiers in Plant Science*, 10.

Legends to figures

Figure 1. Phylogenetic analysis of plant alpha1,3-FucT proteins.

Phylogenetic relationships between plant FucT protein sequences were analyzed using the one click workflow of the https://ngphylogeny.fr/workflows/oneclick/ website (Lemoine, F., Correia, D., et al. 2019). Protein sequences were aligned using the MAFFT alignment tool (Katoh, K. and Standley, D.M. 2013), phylogeny was inferred using PhyML 3.0 (Guindon, S., Dufayard, J.-F., et al. 2010), and the tree was processed in Newick utilities (Junier, T. and Zdobnov, E.M. 2010). FucT11 and FucT12 from *A. thaliana* (pink); FucTA, FuctB, FuctC and FuctD from *N. tabacum* (green); FucT1, FucT2, Fuct3 and FucT4 from *N. benthamiana* (blue).

Figure 2. Identification of Cre-loxP recombination events in *GnTI/FucT*-KO-*Cre* #10.

A. Schematic representation of the T-DNA integrated in the *GnTI/FucT*-KO #10 cell line. The entire T-DNA is flanked by loxP sites for subsequent T-DNA excision with Cre-lox system. B. PCR amplifications were carried out on genomic DNA from indicated cell lines with three different pairs of primers [XylTF and XylTR], [Cas9F and NosR] and [RecF and RecR]. PCR control with water (Ct^-). C. Fifty µg of total proteins isolated from *GnT/FucT*-KO #10 (GF10) and *GnT/FucT*-KO-*Cre* #10-16 (GF10 Cre16) were separated on SDS-PAGE and incubated with anti-Flag M2 Alkaline Phosphatase antibodies.

Figure 3. Genetic characterization of the *GnTI/FucT*-KO-*Cre* #10-16 line.

Sequences of the *FucTA-D* targeted exon 3 were obtained by Sanger sequencing, and the PCR amplicons analyzed using TIDE. The corresponding wild-type sequences are shown above, the three sgRNA target sequences are indicated by colored boxes (site 1: green, site 2: blue, site 3: pink), and the PAM sequences shown in bold.

Figure 4. Expression of NtFucTB-Flag and NtFucTC-Flag in *GnTI/FucT*-KO-*Cre* #10-16 line.

A. Detection of FucTB-Flag and FucTC-Flag by western blotting. Microsomal fractions (25 µg) isolated from *GnT/FucT*-KO-*Cre* #10-16 (Ct 16), *FucTB* (1, 2, 7, 8, 12, 17) and *FucTC* (1, 7, 13, 14, 18) were separated on SDS-PAGE, transferred on PVDF membrane and incubated with anti-Flag M2 Alkaline Phosphatase antibodies. B. Detection of α(1,3)-fucosylated proteins in cellular samples by western blotting. TSP (15 µg) isolated from *GnT/FucT*-KO-*Cre* #10-16 (Ct 16), *FucTB* (1, 2, 7, 8, 12, 17) and *FucTC* (1, 7, 13, 14, 18) were separated on SDS-PAGE, transferred on PVDF membrane and incubated with polyclonal anti-alpha(1,3)-fucose antibodies and secondary anti-rabbit-POD antibodies. C. Detection of alpha(1,3)-fucosylated proteins in extracellular medium by western blotting. Extracellular medium (50 µL) collected by filtration of cultures from wild type BY-2 (wt: dilution 1:50, 1:20), *GnT/FucT*-KO-*Cre* #10 (Ct 10), *GnT/FucT*-KO-*Cre* #10-16 (Ct 16), *FucTB* (1, 2) and *FucTC* (1, 7) were separated on SDS-PAGE, transferred on PVDF membrane and incubated with polyclonal anti-alpha(1,3)-fucose antibodies and secondary anti-rabbit-POD antibodies (left panel). TSP (30 µg) prepared from the corresponding filtrated cells collected were also analyzed (right panel).

Figure 5. **Identification of *N*-glycans.**

MALDI-TOF Mass spectra of 2AB-labelled *N*-glycans extracted from (A) *GnT/FucT*-KO-*Cre* #10-16; (B) FucTC#1; (C) FucTC#7 cell lines cultivated in MS medium after PNGase A (A, B, C1) or PNGase F (C2) treatment. For each sample, the full mass spectrum is presented as well as a zoom panel on narrow *m/z* window showing the presence of an ion of *m/z* 1523.516 corresponding to the $Man5F^3$ *N*-glycan.

Figure 6. Expression of NtFucTB-Flag and NtFucTC-Flag in *XylT/FucT*-KO *N. benthamiana* leaves.

A. Detection of Cas9-Flag in *XylT/FucT*-KO *N. benthamiana* leaves by western blotting. Seventy-five µg of total proteins isolated from wild type *N. benthamiana* leaves or *FucT/XylT*-KO#20-4 *N. benthamiana* leaves were separated on SDS-PAGE and incubated with anti-Flag M2 Alkaline Phosphatase antibodies. B. Detection of FucTB-Flag and FucTC-Flag by western blotting. Microsomal fractions (30 µg) isolated from three FuctB-Flag infiltrated leaves, two FucTC-Flag infiltrated leaves, and one controlled leaf, were separated on SDS-PAGE, transferred on PVDF membrane and incubated with anti-Flag M2 Alkaline Phosphatase antibodies. C. Detection of alpha(1,3)-fucosylated proteins in cellular samples by Western blotting. TSP (50 µg) isolated from three FuctB-Flag infiltrated leaves, two FucTC-Flag infiltrated leaves, and one controlled leaf, were separated on SDS-PAGE, transferred on PVDF membrane and incubated with polyclonal anti-alpha(1,3)-fucose antibodies and secondary anti-rabbit-POD antibodies.

Figure 7. Electrostatic surface representation of NtFucTB/C donor and acceptor binding pockets.

The molecular surface of NtFucTB (A) or NtFucTC (B) is colored from red to blue according to the electrostatic potential using the program PyMol. The GDP-fucose donor and Man5Gn acceptor structures are shown as stick models in the donor and acceptor binding sites, so that the core GlcNAc residue of Man5Gn is positioned correctly according to the GDP-binding site and the catalytic glutamate residue (white). Some amino acids of the acceptor pocket that differ between NtFucTB and NtFucTC are detailed. The inset (C) shows a cartoon representation of the Man5Gn-Asn glycan (with labeling of each monosaccharide) positioned in the active site of NtFucTB (green) and NtFucTC(cyan).

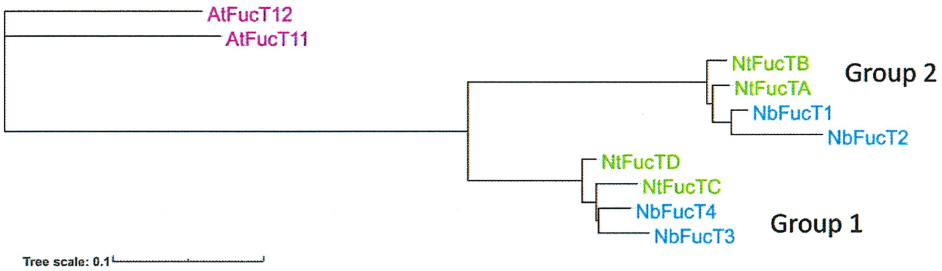

Figure 1. Phylogenetic analysis of plant alpha1,3-FucT proteins.

523x144mm (236 x 236 DPI)

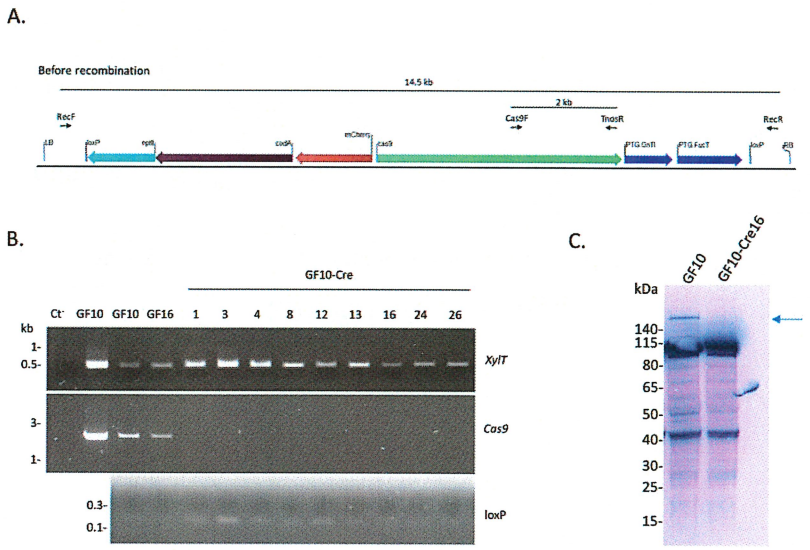

Figure 2. Identification of Cre-loxP recombination events in *GnTI/FucT*-KO-*Cre*#10.

755x533mm (236 x 236 DPI)

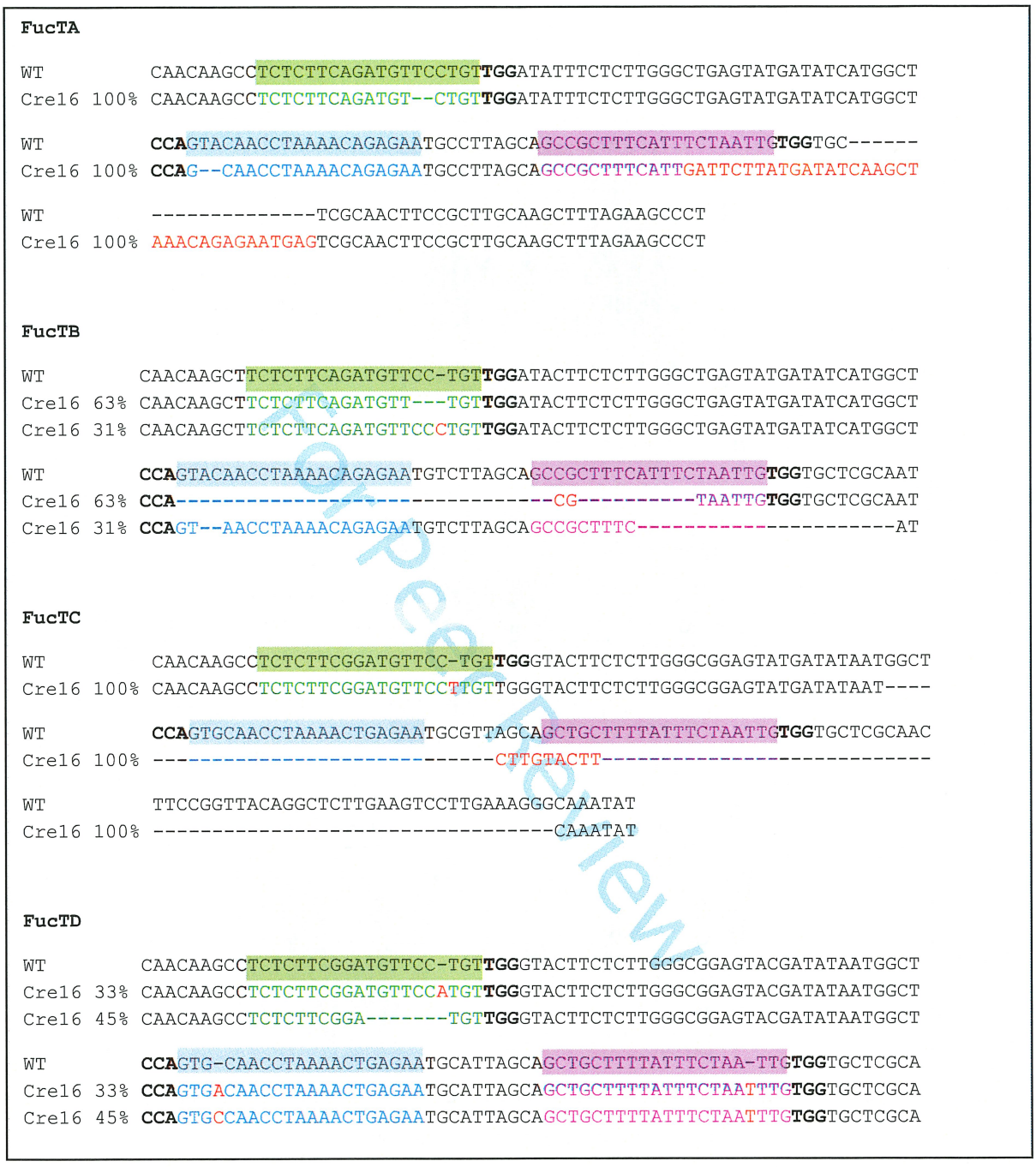

For Peer Review

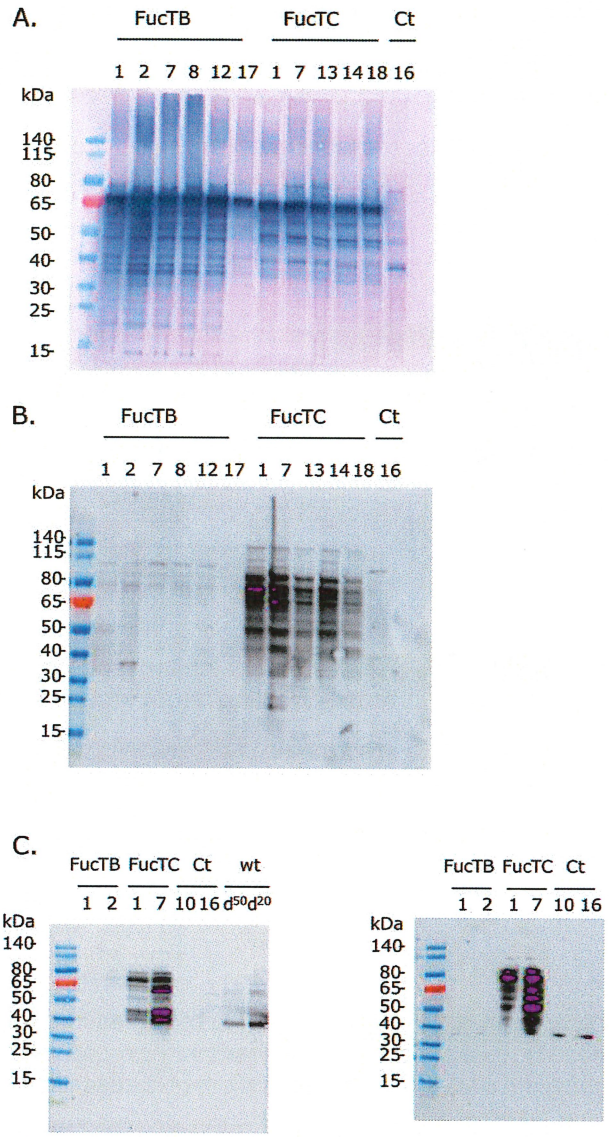

Figure 4. Expression of NtFucTB-Flag and NtFucTC-Flag in *GnTI/FucT*-KO-*Cre*#10-16 line.

493x915mm (236 x 236 DPI)

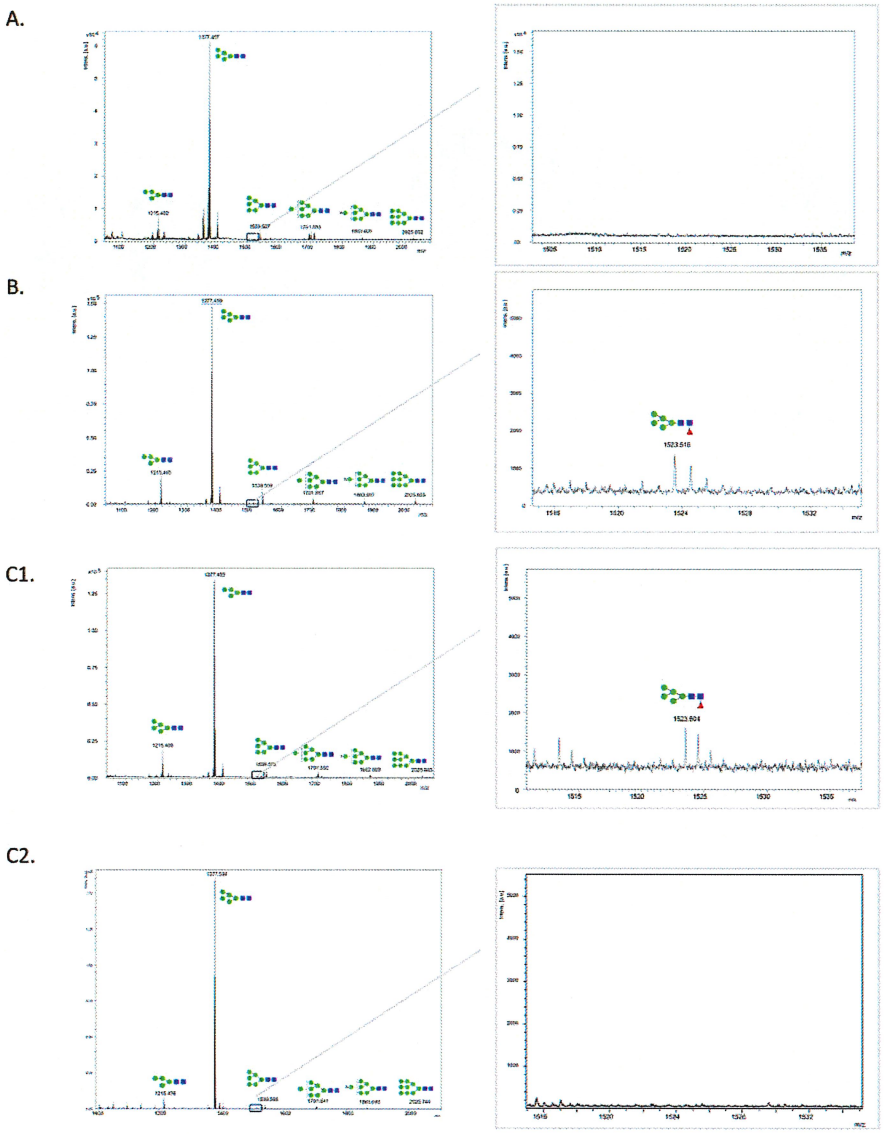

Figure 5. Identification of *N*-glycans.

600x767mm (236 x 236 DPI)

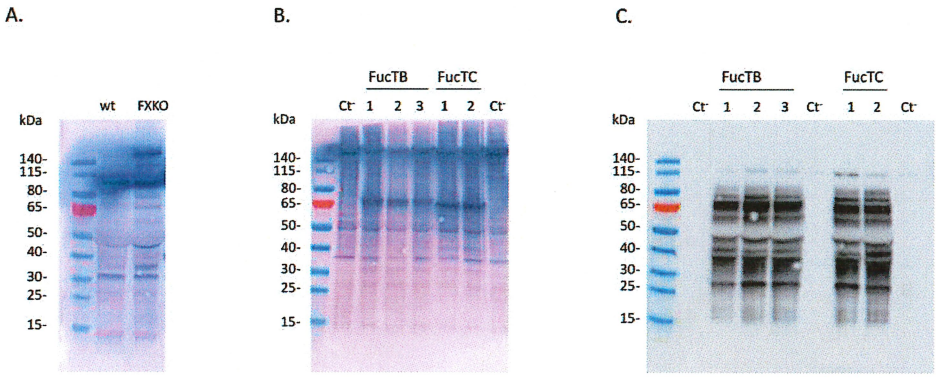

Figure 6. Expression of NtFucTB-Flag and NtFucTC-Flag in *XylT/FucT*-KO *N. benthamiana* leaves.

628x243mm (236 x 236 DPI)

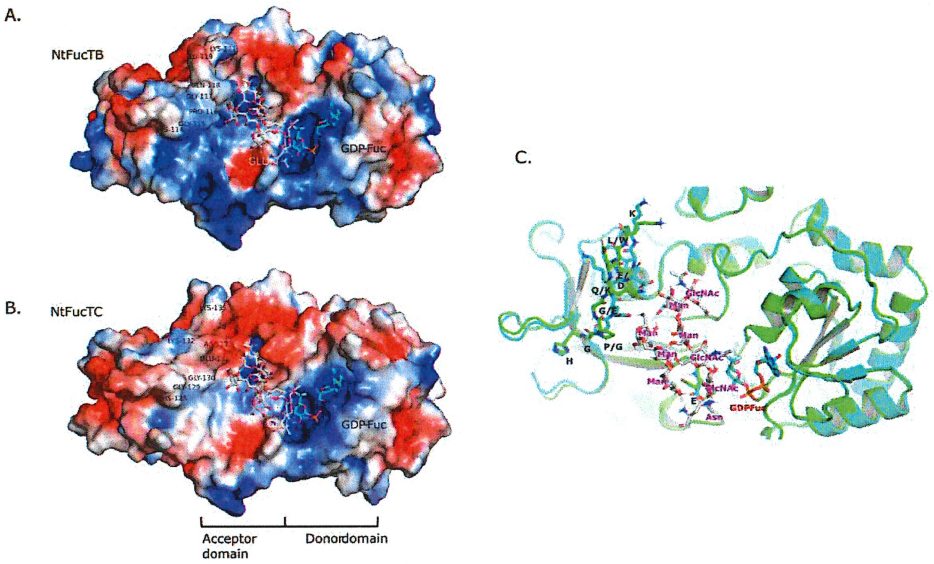

Figure 7. Electrostatic surface representation of NtFucTB/C donor and acceptor binding pockets.

716x425mm (236 x 236 DPI)

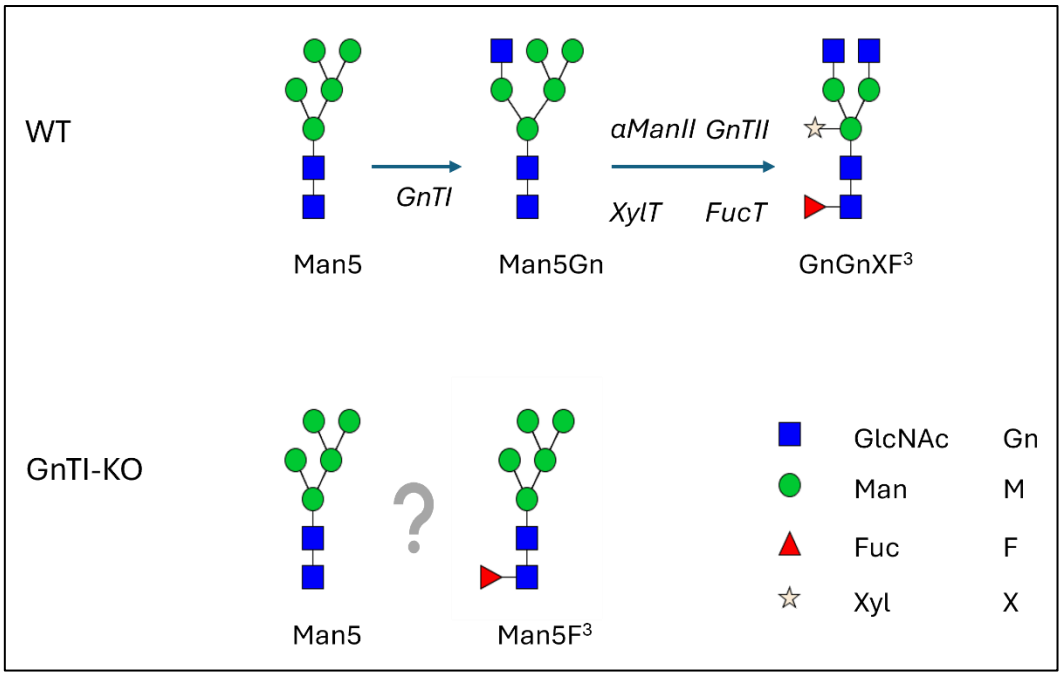

Supplementary Figure 1. Graphic representation of genes involved in maturation of Man5 *N*-glycan in plant cells.

Monosaccharide symbols follow the SNFG system (Glycobiology 25:1323-1324, 2015). *N*-glycan nomenclature follows Beilstein J Org Chem 20: 607-620, 2024.

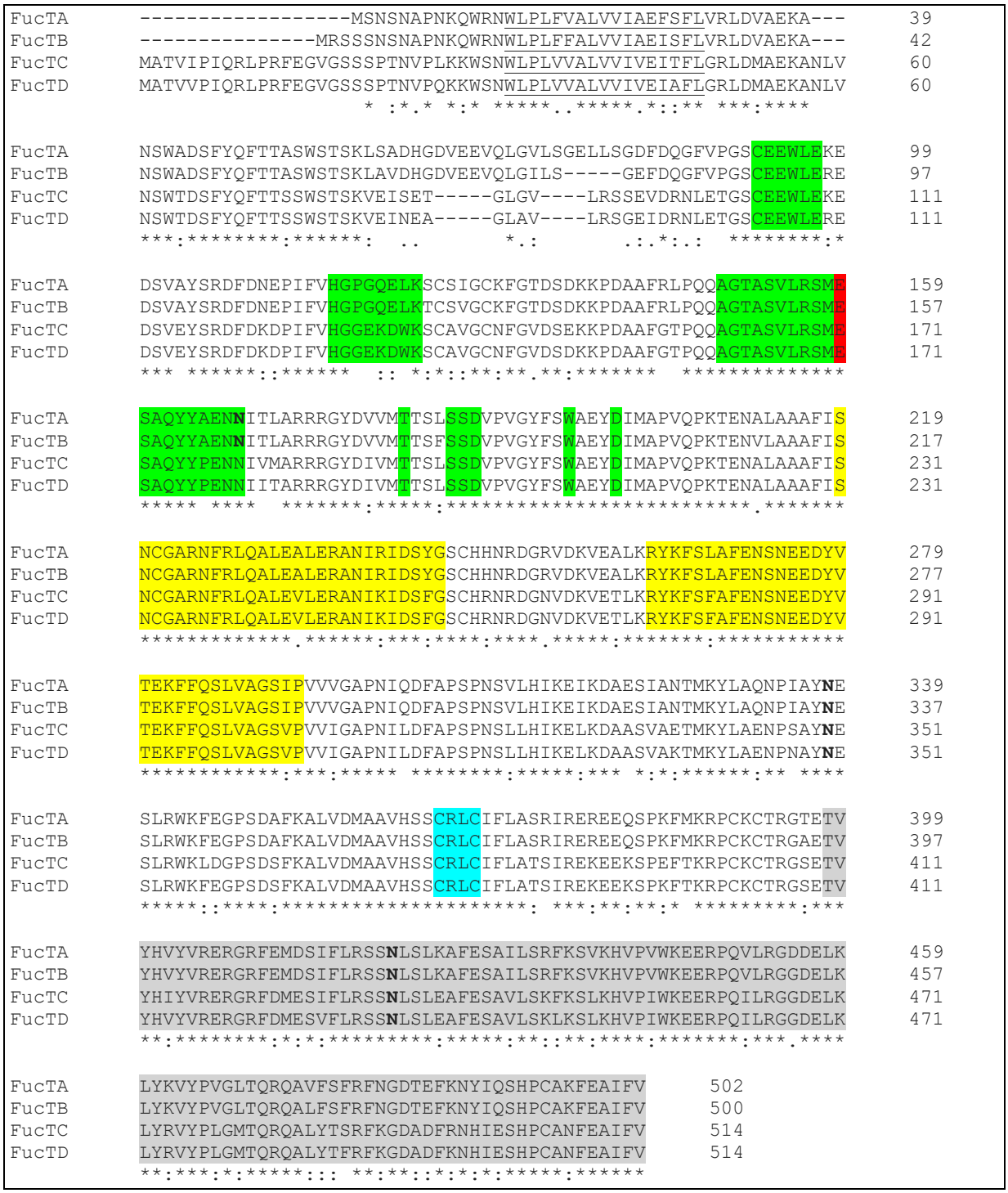

Supplementary Figure 2. Alignment of *Nicotiana tabacum* alpha1,3-FucT proteins.

CLUSTAL O (1.2.4) multiple sequence alignment of *N. tabacum* FucTA/B/C/D protein sequences. The transmembrane domain is underlined. In red, the catalytic base Glu; in grey, the plant alpha1,3- FucT C-terminal region of ~110 residues; in blue, CXXC motif involved in the formation of intramolecular disulphide bonds that delineate the catalytic domain; in yellow, the "1st cluster" and the "alpha1,3-FucT motif" characteristic of the GT10 family form the catalytic GDP-L-fucose donor domain; in green, residues that are conserved in plant alpha1,3-FucTs and that might play a role in the discrimination of acceptor substrates; in bold the putative N-glycosylation sites.

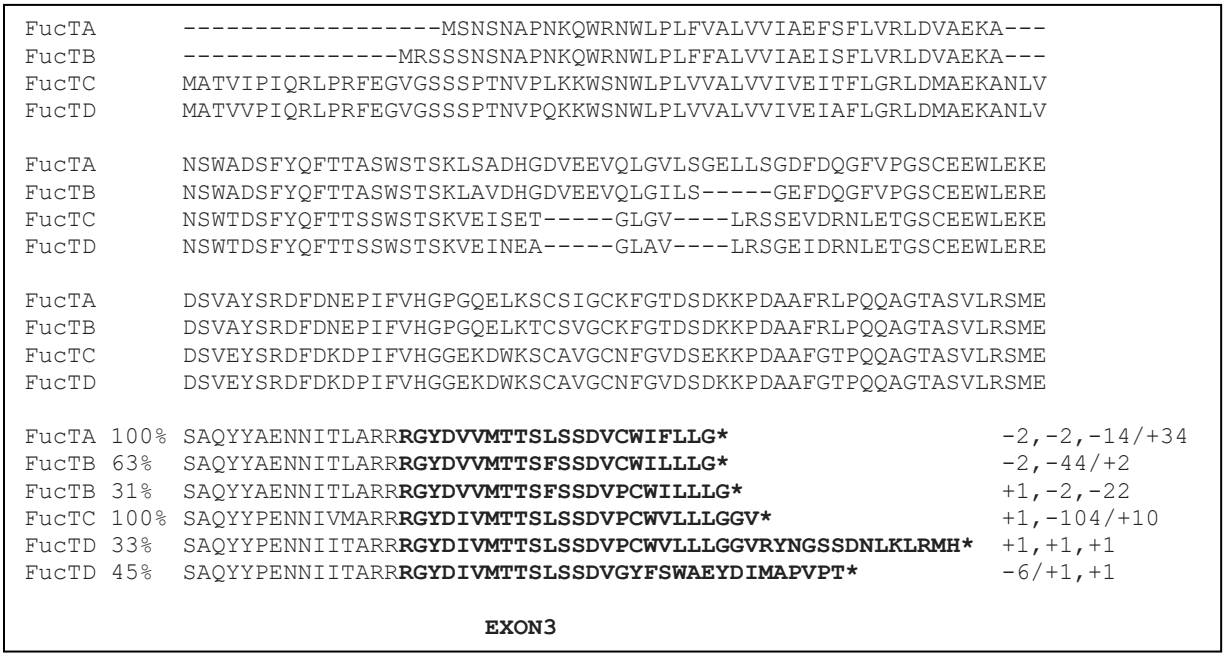

Supplementary Figure 3. Protein sequences of truncated alpha1,3-FucTs in the *GnTI*/*FucT*-KO-*Cre* #10-16 line.

The residues corresponding to the EXON3, which was targeted by CRISPR/Cas9, are in bold. Premature Stops are marked by an asterisk.